Climate change is rapidly deteriorating the climatic signal in Svalbard glaciers

Andrea Spolaor[1,2], Federico Scoto[3,2], Catherine Larose[4], Elena Barbaro[1,2], Francois Burgay[5,2], Mats P. Bjorkman[6], David Cappelletti[7], Federico Dallo[2], Fabrizio de Blasi[1,2], Dmitry Divine[8], Giuliano Dreossi[1,2], Jacopo Gabrieli[1,2], Elisabeth Isaksson[8], Jack Kohler[8], Tonu Martma[9], Louise S. Schmidt[10], Thomas V. Schuler[10], Barbara Stenni[2], Clara Turetta[1,2], Bartłomiej Luks[11], Mathieu Casado[12] and Jean-Charles Gallet[8].

[1]CNR-Institute of Polar Science (ISP), Campus Scientifico, Via Torino 155, 30172, Venice-Mestre, Italy.
[2]Department of Environmental Sciences, Informatics and Statistics, Ca' Foscari University, Venice, Italy
[3]Institute of Atmospheric Sciences and Climate, ISAC-CNR. Campus Ecotekne, 73100 Lecce, Italy
[4]Institut des Géosciences de l'Environnement (IGE), Université Grenoble Alpes, CNRS, IRD, Grenoble INP, Grenoble F-38000, France
[5]Paul Scherrer Institute, Laboratory of Environmental Chemistry (LUC), 5232 Villigen PSI, Switzerland
[6]University of Gothenburg, Department of Earth Sciences, Box 460, 40530 Göteborg, Sweden
[7]Dipartimento di Chimica, Biologia e Biotecnologie, Università degli Studi di Perugia, 06123 Perugia, Italy
[8]Norwegian Polar Institute, Tromsø NO-9296, Norway
[9]Department of Geology, Tallinn University of Technology, Ehitajate tee 5, 19086 Tallinn, Estonia
[10]University of Oslo, Department of Geosciences, Oslo, Norway
[11]Institute of Geophysics, Polish Academy of Sciences, Księcia Janusza 64, 01-452 Warsaw, Poland
[12]Laboratoire des Sciences du Climat et de l'Environnement, CEA–CNRS–UVSQ–Paris-Saclay–IPSL, Gif-sur-Yvette, France

Corresponding author: andrea.spolaor@cnr.it

Abstract

The Svalbard archipelago is particularly sensitive to climate change due to the relatively low altitude of its main ice fields and its geographical location in the higher North Atlantic, where the effect of the Arctic Amplification is more significant. The largest temperature increases have been observed during winter, but increasing summer temperatures, above the melting point, have led to increased glacier melt. Here, we evaluate the impact of this increased melt on the preservation of the oxygen isotope signal ($\delta^{18}O$) in firn records. $\delta^{18}O$ is commonly used as proxy for past atmospheric temperature reconstructions and, when preserved, it is a crucial parameter to date and align ice cores. By comparing four different firn cores collected in 2012, 2015, 2017 and 2019 at the top of the Holtedahlfonna ice field (1100 m. a.s.l.), we show a progressive deterioration of the isotope signal and we link its degradation to the increased occurrence and intensity of melt events. Our findings indicate that starting from 2015, there has been an escalation in melting and percolation resulting from changes in the overall atmospheric conditions. This has led to the deterioration of the climate signal preserved within the firn or ice. Our observations correspond with the model's calculations, demonstrating an increase in water percolation since 2014, potentially reaching deeper layers of the firn. Although the $\delta^{18}O$ signal still reflects the interannual temperature trend, more frequent melting events may in the future affect the interpretation of the isotopic signal, compromising the use of Svalbard ice cores. Our findings highlight the impact and the speed at which Arctic Amplification is affecting Svalbard's cryosphere.

Introduction

Arctic regions are undergoing faster warming than the global average, due to the so-called “Arctic Amplification”(Serreze and Barry, 2011). Arctic Amplification is caused by various feedback processes in the atmosphere-ocean-ice system and significantly affects the Arctic North Atlantic region. Arctic warming is not seasonally uniform and has the largest impact in the winter months and close to the surface (Dahlke and Maturilli, 2017). Furthermore, it is not evenly distributed across the Arctic; the largest warming rates are over the Barents/Kara Seas, where autumn and winter sea-ice retreat is the most pronounced (Lind et al., 2018; Isaksen et al., 2022, 2016). However, even at tropospheric levels, there is a significant warming signal in recent decades that peaks in the Svalbard region, and more generally, in the North Atlantic sector of the Arctic (Dahlke and Maturilli, 2017). Rates there are up to four times the global average since 1979 (Rantanen et al., 2022b).

Glaciers and ice caps in the Svalbard archipelago cover an area of ~34,000 km^2, representing about 6% of the world’s glacier area outside the Greenland and Antarctic ice sheets. Svalbard glaciers contain 7740 ± 1940 km^3 (or Gigaton; Gt) of ice, sufficient to raise global sea level by 1.7 ± 0.5 cm if

totally melted (Schuler et al., 2020; Geyman et al., 2022; van Pelt et al., 2019). As a result of both Arctic Amplification and their peculiar position at the edge of Arctic sea ice retreat, they are experiencing among the fastest warming on Earth (Noël et al., 2020).

Ongoing climate trends also affect the state of the seasonal snowpack in Svalbard (Østby et al., 2017; van Pelt et al., 2016), with the number of days with snow-cover on the ground in Longyearbyen decreasing from 253 (1976-1997) to 219 (2006-2018) (data from Monitoring of Svalbard and Jan Mayen, mosj.no). The change in the Svalbard climate also has strong repercussions for the entire environment of the archipelago, leading to an increase in frequency of Rain on Snow (RoS) events (Wickström et al., 2020; Salzano et al., 2023) which lead to pervasive ice layers(Sobota et al., 2020) covering the ground, limiting access to food for reindeers (Peeters et al., 2019). It has also led to a reduction in sea ice that is limiting and changing the hunting area of polar bears. These changes over time might be captured in ice core records. Ice cores are commonly used to derive information about past climate conditions and atmospheric composition, including traces of natural events such as volcanic eruptions (Sigl et al., 2014), anthropogenic contamination(Vecchiato et al., 2020)and past temperature variability (Wolff et al., 2010), revealing that abrupt climate changes have repeatedly occurred over the last ice age. For example, during the so-called Dansgaard-Oeschger events, temperatures rose by about 5°C within centuries (Boers, 2018). However, even during these natural abrupt events, a complete transition from stadial (glacial) to interstadial (warm) conditions took about a century (Scoto et al., 2022; Steffensen et al., 2008). Current temperature rise in Svalbard is much faster than the one observed during the D-O events, with the annual mean surface air temperature increasing on average by $+1.3\ °C \pm 0.7\ °C$ per decade, and winter mean temperature increasing by $+3.1 \pm 2.4\ °C$ per decade (Dahlke et al., 2020; Maturilli et al., 2013).

Snowmelt and water percolation at the sampling site can move the chemical constituents across the layers (Spolaor et al., 2021; Avak et al., 2019) disturbing the original signal. Prolonged events can even fully compromise the preservation of the climatic information contained by ice cores. Avak et. al., (2019) showed that atmospheric composition was well preserved in an Alpine ice core during the winter, but that the melting in the spring and early summer caused a preferential loss of certain major ions and trace elements. In particular, the elution behavior of major ions is most likely controlled by redistribution processes occurring during snow metamorphism, as underlined by recent work investigating the distribution of impurities within the ice matrix (Bohleber et al., 2021). Variable mobility has also been observed for trace elements, although they have been suggested to be better preserved than major ions (Avak et al., 2019). Since the temperature is below the melting point (<0°C) throughout the year, the Antarctic and the Greenland plateaus are the best locations for such studies, nevertheless, rare melting events have been observed in the Greenland plateau (Bonne et al., 2015).

Beyond the polar regions, many other drilling sites have been investigated including the Alps (Arienzo et al., 2021; Gabrielli et al., 2016; Schwikowski et al., 1999), the Himalayas (Thompson et al., 2018; Dahe et al., 2000), the Andes mountain range (Hoffmann et al., 2003; Thompson et al., 2021), the Canadian Arctic (Zdanowicz et al., 2018) and the Svalbard archipelago (Isaksson et al., 2005; Wendl et al., 2015) to reconstruct the past atmospheric and climate condition as well as the anthropogenic contamination (Vecchiato et al., 2020) in different and specific regions of the Earth.

There are several ice caps in Svalbard, but given their relatively low altitude, most are not suitable for the preservation of a pristine climate archive. The glacier equilibrium line altitude (ELA) varies across the different regions of the archipelago, but is generally situated between 300 to 700 m a.s.l.(van Pelt et al., 2019). In the southern part of the archipelago, the ELA is lower due to the higher winter snow accumulation, while in the northern part, the ELA rises to 600-700 m. Signal preservation requires drilling to be above the ELA for regular snow accumulation, but also, so that summer percolation only moderately affects the upper firn layers.

Several drilling operations have collected ice core records in the Svalbard archipelago. The longest ice-core record (in time coverage) was collected from Lomonosovfonna, at 1230 m a.s.l., and covered ~1200 years of Svalbard climate history (Divine et al., 2011) and was used in conjunction with a more recent core drilled in Holtedahlfonna (1140 m a.s.l.) that covered the past 300 years to reconstruct past winter surface air temperature for Svalbard based on isotopic analysis (Divine et al., 2011). The authors were able to identify three major sub-periods providing valuable insights into the historical temperature variations in Svalbard from this ice core. The first period, spanning from 800 to 1800, was characterized by a continuous decline in winter temperatures that occurred at a rate of about 0.9 °C per century. The second period that occurred during the 1800s was the coldest century in Svalbard, with a winter cooling of 4°C relative to the 1900s associated with the Little Ice Age. Finally, based on the reconstructed temperature data, the authors identified a third period characterized by rapid warming and the reduction in sea-ice extent as of the beginning of the 1900s. These findings highlight the validity of using isotope data for temperature reconstructions.

Other Svalbard ice cores have also been retrieved from Austfonna (750 m. a.s.l.), covering approximately 900 years and Vestfonna (600 m a.s.l.) covering approximately 500 years, and showed that most of the chemical constituents contained in the initial snow cover remained in the ice cores, although melt water percolation had led to their re-distribution (Watanabe et al., 2001) (Matoba et al., 2002). The Holtedahlfonna ice core was also used to study major ions (Beaudon et al., 2013) and when compared to the Lomosonosovfonna core, the obtained record suggests that there are local influences affecting the studied chemical species, possibly related to the proximity of the Greenland Sea. In addition, east–west disparities between the cores were also apparent and were attributed to

different air mass sources for these two regions of the Svalbard Archipelago. Although part of the signal variability of the Svalbard ice core was attributed to summer melting, a multi-year resolution environmental record was preserved, likely due to the formation of thin ice layers in the annual snowpack, which act as barriers to the deeper elution of ions. However, all these cores were recovered in late 90s or early 2000s when the temperature rise due to Arctic Amplification was less extreme and the current state of these ice caps and their validity for climate reconstruction is unknown.

In addition to deep-drilling, numerous investigations using shallow ice cores from the Holtedahlfonna have consistently highlighted the site's significance for climate research (Burgay et al., 2021; Barbaro et al., 2017; Ruppel et al., 2017). In light of the Arctic Amplification, Svalbard glaciers and the climate signal they provide are in danger of being degraded, and their reliability for future climate studies needs to be assessed. In order to do so, we conducted oxygen isotopic composition ($\delta^{18}O$) analysis on a series of four shallow ice cores collected at the summit of the Holtedahlfonna ice field. These ice cores were obtained in different years and cover overlapping atmospheric deposition periods, offering insights into the evolution of isotopic stratigraphy over time. In this paper, we focused on $\delta^{18}O$ because it is a widely utilized parameter in ice core science for reconstructing past temperature changes (Divine et al., 2011; Stenni et al., 2017) and it is comparatively less influenced by melting and percolation events (Pohjola et al., 2002) than other chemical parameters analyzed in ice cores. We compared the $\delta^{18}O$ signals among the different shallow cores and discuss the impact of summer melting and meteorology using glacier mass balance measurements and snowpack modeling.

2. Methodology

2.1 The Holtedahlfonna ice field

Holtedahlfonna (HDF – Figure 1) is the largest ice field (ca. 300 km^2) in northwestern Spitsbergen, located about 40 km from the Ny-Ålesund research station. It covers an elevation range of 0–1241 m a.s.l. (Nuth et al., 2017) and the upper part of the glacier, located approximately at 1100 m a.s.l., has a positive annual snow mass balance, ca. +0.50 m. w.e. a^{-1}(van Pelt et al., 2019). The site has already been studied for long term paleoclimate reconstruction, covering the past 300 years (Divine et al., 2011; Goto-Azuma et al., 1995). In April 2005, a 125 m a long ice core was drilled using an electromechanical corer and the bottom temperature in the borehole was –3.3°C, assuring cold ice conditions over the entire ice thickness. Ice temperature measured in the borehole featured a maximum of –0.4°C at 15 m depth, indicative of firn-warming due to the release of latent heat from refreezing (Beaudon et al., 2013).

2.2 The Holtedahlfonna shallow firn cores: collection and processing

In the spring seasons of 2012, 2015, 2017 and 2019, a total of four shallow cores were obtained from the summit of the Holtedahlfonna ice field (79°09′N, 13°23′E; 1150 m. a.s.l.). The shallow cores were collected using a 4″ fiberglass Kovacs Mark-II ice corer driller powered by an electric drill and reached depths of 7-10 m into the firn. All shallow cores were drilled from the bottom of the annual snowpack\last summer surface. Length and density of each firn core section were logged, stored in plastic sleeves, and transported back to Ny-Ålesund for laboratory analysis. For cores collected in 2012, 2017 and 2019, core samples were processed in a class-100 laminar flow hood in the laboratory of the Italian research station "*Dirigibile Italia*" in Ny-Ålesund. Core sections were cut into pieces of 5 to 7 cm length using a ceramic knife and the external part of the core physically removed to avoid contamination. The density was measured for each sample produced. The core 2015 was processed as reported in Ruppel et al. (2017).

2.3 Oxygen stable isotope analysis ($\delta^{18}O$)

The samples for oxygen isotopic analyses ($\delta^{18}O$) were melted at room temperature (≈20°C) and transferred into 2-mL clear glass vials filled to the top. Samples were kept refrigerated at +4°C and analyzed at Ca Foscari University of Venice (2017 and 2019) and at Tallinn University of Technology (2012 and 2015). In both cases, the isotopic measurements were carried out using a Picarro L1102-*i* analyser coupled with a CTC Pal autosampler. The instrument uses Cavity Ring-Down Spectroscopy (CRDS) technology, based on the unique near-infrared absorption spectrum of each gas-phase molecule. The autosampler injects the melted sample into the vaporizer (set at 110°C), where it becomes gaseous and is then transferred into the cavity (nitrogen is used as a carrier), in which the measurement occurs. The instrument datasheet reports an analytical precision of ± 0.10 δ‰ for $\delta^{18}O$. Each sample was injected eight times: only results within ± σ from the 8-repetition average were kept for records, while outliers were discarded. Internal isotopic standards periodically calibrated against IAEA-certified standards (V SMOW 2 and SLAP 2) were used for calibration.

2.4 Holtedahlfonna surface mass balance

Surface mass balance (SMB) of Holtedahlfonna is monitored by the Norwegian Polar Institute (Kohler, 2013). SMB is obtained from repeated field visits at the end of winters and summers, with winter snow-depth sounding and density measurements and repeated height readings of an array of stakes along the glacier centerline. Balance estimates are extrapolated over the entire glacier basin by determining the balance as function of elevation and averaging them, applying weights determined from the distribution of glacier area as a function of elevation. This method quantifies the glacier-wide SMB, i.e., the mass changes at the surface of the glacier, and within near-surface layers, but

does not include internal mass changes below the last summer surface. SMB measurements at Holtedahlfonna started in 2003; since the drilling site is in the accumulation area, these measurements provide information of the seasonal accumulation, but disregard the internal accumulation that may occur due to refreezing of meltwater in layers below the last summer surface. The uppermost part of HDF has had a consistently positive mass balance and is therefore assumed to preserves most of its annual snow deposition.

2.5 Estimation of Meteorological condition at the summit of the Holtedahlfonna ice field

In absence of in-situ meteorological measurements at the drill site, we obtained long-term seasonal (DJF, MAM, JJA and SON) temperature and precipitation series from the high-resolution CARRA dataset (Copernicus Arctic Regional Re-Analysis, Schyberg et al., 2020). This 2.5 km resolution product covering the period 1991-2020 is downscaled from ERA5(Hersbach et al., 2020) using the state-of-the-art weather prediction model HARMONIE-AROME (Bengtsson et al., 2017). CARRA has several improvements compared to ERA5, including assimilation of a large amount of additional surface observations, use of satellite data, and improved representation of sea ice; it is therefore likely to provide the best estimate of meteorological conditions in the Barents Sea region.

The CARRA reanalysis is also used to force the CryoGrid community model (Westermann et al., 2023) to simulate glacier mass balance, seasonal snowpack evolution and meltwater runoff across Svalbard Franz-Joseph Land and Novaya Zemlya. The model couples the surface energy balance and a multi-layer subsurface module to resolve meltwater production, percolation, storage, refreezing and runoff, accounting for the interaction with local density and temperature stratigraphers. The vertical discretization comprises 47 layers of variable vertical extend to cover the uppermost 20 m below the surface (Steffensen Schmidt et al., 2023).

3.RESULTS

3.1 Shallow firn core dating and alignment

To date the core, we use the seasonal cycle (where present) of the $\delta^{18}O$ data together with the mass balance data available since 2003. Core depths were converted to water equivalent using the density data acquired during the core processing. Density for the 2015 core is taken from Ruppel et al., (2017), the 2012 values are published in (Spolaor et al., 2013), and density for the 2017 and 2019 cores are presented in this work; density profiles of the four shallow cores (Figure S1) all reveal a similar pattern.

The cores were collected within 50 m of the mass balance stake HDF-10. The stake measurements, which show a consistently net positive mass balance (Figure 2), provide a historical record of

snowpack accumulation that can be directly used to assign a specific year to firn core depth range (Figure 3).

Oxygen stable isotopes can be used independently to annually date the ice, but only in ice-core archives where the seasonal signal is well preserved. This means that snow accumulation needs to be sufficiently high, and the summer ablation should not compromise the stratigraphy by redistributing and smoothing the original atmospheric signal. By combining the annual accumulation and the core depth expressed in water equivalent and the seasonality of $\delta^{18}O$ (where available and preserved), we can date and align all four cores (Figure 3).

The cores cover 14 years in total (from 2005 to 2018). The time coverage for each core is reported in Table 1 together with additional information for each firn core. The 2012 core had a $\delta^{18}O$ average value of -15.3 ± 1.0 ‰, the 2015 core a value of -15.1 ± 0.8 ‰, the 2017 core an average value of -14.4 ± 0.7 ‰ and the 2019 core an average value -14.1 ± 1.2 ‰. Specific features overlap in the four cores (Figure 3 and 6), and show a general increasing trend in $\delta^{18}O$ from 2005 until 2018. In particular, the 2012 and 2015 cores have similar fluctuations with shared features, particularly during 2005-2006, which was used for core alignment. They also showed similar features in the remaining periods that they each covered, though with minor differences. The high $\delta^{18}O$ values in 2013 that occurred in the 2015 core are also clearly found in the 2017 core, helping to synchronize the records. The alignment of the 2019 core with previous cores could only be done through mass balance values, since the $\delta^{18}O$ values did not show the same peaks as the other records. In particular, the decrease in $\delta^{18}O$ values recorded in the period representing 2016 was not present in the 2017 core.

3.2 Meteorological condition at the Holtedahlfonna ice field summit

The meteorological conditions at the Holtedahlfonna ice field summit from 1991 to 2019 were retrieved from model re-analysis and provide a clear overview of the on-going changes occurring at the site.

The annual average winter temperatures (DJF) at the HDF summit (located at 1100 m a.s.l.) ranged from -25°C to -15°C, and show an increasing trend of 2.37°C per decade for the period 1991–2019 (Figure 4a - blue line). The annual average spring and summer temperatures (MAM) ranged from -17°C to -12°C (Figure 4a - green line) and -5°C to -1°C (Figure 4a - red line), respectively. The average temperature increase per decade since 1991 was 0.38°C for spring and 0.51°C for summer. The temperature during fall (SON) increased by 1.47 °C per decade and ranged from -15°C and -5°C (Figure 4a - brown line).

Although the average seasonal summer temperatures were below the water melting point, positive degree days (PDD – Figure 4b, expressed as the sum of mean daily temperatures for all days during

a period where the temperature is above 0°C), occurred at the summit of HDF, causing snowpack melting. The cumulative annual PDD, retrieved from model temperature series outputs, showed a stable value for the period 1990 to 2015, although some years (1994, 1999, 2010) and periods (2001–2006) were characterized by an increased PDD. A net increase from 2015 to the present time was recorded. Snow melting at the site was clearly visible and confirmed by the presence of several ice lenses in the core (Spolaor et al., 2013; Burgay et al., 2021).

The annual model estimated precipitation (1991–2019) ranged between 630 to 1170 mm w.e. per year, with a slight increase in the most recent period (Figure 4d). A similar trend was also observed in Ny-Ålesund (Førland et al., 2020). Seasonal precipitation (Figure S2) was most abundant during fall (SON) and winter (DJF), with an average precipitation of 286 mm w.e. and 274 mm w.e, respectively, and a relative average contribution of 32% and 31%, respectively, to the total deposition. The lowest precipitation occurred in spring (MAM) and summer, with an average precipitation of 170 mm w.e. and 145 mm w.e., respectively, which represents an average contribution of 20% of the total deposition in spring and 17% of the total precipitation in summer.

Although the annual mass balance was always positive, the summer mass balance was both positive and negative depending on the meteorological conditions (Figure 2). The winter accumulation represented between 60% and 100% of the net annual mass balance at the site. Even though the summer mass balance data from 2015 to 2020 were positive, melting also occurred and water percolated into the snow and firn before refreezing.

Most of the melting occurred during the summer period (JJA), but melting events also occurred during fall and late spring (Figure S3). The estimated annual melting at the site from 1991-2020 (Figure 4c) varied between 960 mm w.e (2020) and 117 mm w.e (2008) and showed a clear increasing tendency following temperature rise. Moreover, autumn snowpack melting events, previously rare, became a more regular phenomenon in the period 2015 to 2019. However, spring snowmelt is sporadic (2011) and rare.

In addition to meteorological reanalysis from the HARMONIE-AROME model, the CryoGrid simulation provided information about the presence of liquid water in the firn and its penetration (Figure 5). Percolation was mainly confined to the surface layer between 1991 (beginning of the simulation) to the end of the 90s(except 1999). Percolation increased significantly from 2000 onwards. In particular, for the period 2004-2005, severe surface melt events occurred (Figure 2c and Figure S3), causing water percolation for several meters (Figure 5). The 2006 to 2014 period was characterized by relatively limited surface melting and the lowest amount of percolated water, which did not exceed one (2006 and 2008) to four (2010 and 2011) annual snow accumulation periods. Based on the model's calculations, water percolation increased since 2014 and was able to reach

deeper firn strata. Although the model suggests the presence of liquid water in the firn, water and elution channels are complex to simulate and likely present high spatial variability. Hence, we only consider the data presented in Figure 5 in a qualitative manner to evaluate the possible presence or absence of liquid water within the snowpack and its theoretical penetration\percolation depth.

4. DISCUSSION

The aim of this paper is to evaluate the effect of temperature rise on the $\delta^{18}O$ Holtedahlfonna ice core signal preservation. Our discussion will focus only on the periods covered by the shallow cores.

Based on the $\delta^{18}O$ records of the four shallow cores, it is evident that the seasonal signal for the core 2019 and 2017 experienced considerable changes and progressively deteriorated. While wind redistribution can transport snow, it primarily affects snow deposited at similar altitudes, which tends to have a similar water stable isotope fingerprint. It is highly improbable that snow deposited at lower elevations could be lifted and deposited at the summit of Holthedalfonna in quantities sufficient enough to completely degrade the climate signal preserved in the ice. Moreover, analysis of wind patterns in Ny-Ålesund does not indicate any significant shifts or changes in average wind velocities (Cisek et al., 2017).

We hypothesize that the most important parameters affecting the pristine atmospheric signal trapped in the snow is the amount of snow melting, which depends on the snow and meteorological conditions, and the penetration of the melt water into the snowpack.

In the core collected in 2012 (Figure 3), the seasonal variations are clear for almost the entire period except for 2004-2005, a period characterized by significant summer melt that disturbed the atmospheric signal trapped in the ice. However, for the period 2006-2011, the seasonality is clear and each $\delta^{18}O$ seasonal cycle is confined within the annual snow mass balance measurements.

The 2015 core still presented the seasonal cycle in the upper half of the core, corresponding to the second period (2010-2014). However, the seasonal feature of the $\delta^{18}O$ identified in the 2012 core for the periods 2008–2009 was no longer present, suggesting a possible elution caused by the percolation of liquid water (Figure 5). The model simulation supports the possibility that post deposition events may have occurred within the firn due to the percolation of liquid water.

The most striking change in terms of the $\delta^{18}O$ seasonal cycle occurred in the 2017 core. The 2017 core overlapped with the 2015 core for the period 2012-2014 and, while the seasonality for this period was well defined in the 2015 core, only the seasonal $\delta^{18}O$ for year 2013 was visible in the 2017 core. The $\delta^{18}O$ seasonal cycle of 2014 has undergone significant smoothing and the $\delta^{18}O$ seasonal cycle in 2012 is no longer visible. For the period 2015-2016, the seasonal cycle was not clear, although oscillations were still present.

In the most recent core collected in 2019, a seasonal $\delta^{18}O$ cycle could no longer be detected and particular features, such as the drop in the $\delta^{18}O$ signal in 2016 (not observed in the 2017 core), was not linked to a drop in the temperature, since 2016 was the warmest year on record (Figure 6, red dots).

Two independent statistical analyses, one using the significant value of a regression model and the other using the spectral analysis, were performed on the shallow core records to test the presence of seasonal oscillation on the $\delta^{18}O$ signal. Both statistical analyses demonstrated the disappearance of the seasonal signal in the most recent (2017 and 2019) shallow cores (full details are reported in the supplementary material - section 2). Using the linear regression model for each core and each year, we first identified the maximum and the minimum for the $\delta^{18}O$ signal (Figure 6) and then calculated the weighted slope between each extreme value (Figure 7). We determined the annual maximum and minimum values by referencing the annual mass balance dating for individual shallow cores (Figure 3). Specifically, within the time windows defined by the mass balance values, we pinpointed the extreme values closest to the start or conclusion of the glaciological year, while adhering to the alternating pattern between maximum and minimum values. The significant values of the seasonality of the weighted slope considering the increasing and decreasing periods separately is presented in Table S1. A significant seasonality (p-value < 0.05) is only observed in 2012 and 2015 ice cores.

The change in the seasonal patterns of precipitation, and to a lesser degree, the overall quantity, could have influenced the $\delta^{18}O$ signal of the four cores. However, from the model results, the seasonal contribution to the total annual precipitation did not change significantly (Figure S2). This would suggest that precipitation does not play a central role in explaining the degradation, or possible change, in the $\delta^{18}O$ signal, and that increased melting and water percolation might have had a larger effect. Instead, the increase in year-round precipitation could enhance melt water formation during the summer periods. The preservation of the ice core climate signal strongly depends on the amount of snow melt during summer and the capability of water to penetrate the snowpack, which in turn is controlled by snow temperature. The progressive atmospheric warming, the increase of summer melting and water percolation as well as the water movement within the snowpack could all have had an impact on the $\delta^{18}O$ signal present in the Holtedahlfonna firn\ice.

The progressive degradation and loss of the seasonality of the $\delta^{18}O$ signal in the shallow core (2004 - 2018) is also supported by the results obtained from the $\delta^{18}O$ signal in the 2005 core. In the deep core collected in 2005, the seasonal signal of the $\delta^{18}O$ in the period 1960 to 2000 was well preserved (Figure S5). The signal determined in the 2005 Holtedahlfonna deep ice core shared similar features with those determined in the 2012 and 2015 shallow cores, where the seasonal oscillations were still partially present, but not with signals determined in the 2017 and 2019 cores, where the seasonality

in $\delta^{18}O$ almost disappeared. We suggest that since 2015, estimated melting and percolation increased because of the evolution of the general atmospheric conditions, causing a deterioration of the climate signal preserved in the firn\ice.

Water stable isotopes are commonly used as a temperature proxy. By overlapping the water stable isotope profiles measured in the shallow cores and, comparing their trends with the annual average temperature, we suggest that the general atmospheric temperature trend is still preserved within the HDF ice (Figure 8), although some clear deterioration is visible. For example, the highest annual temperature values recorded in 2016 were not mirrored in the $\delta^{18}O$ record from the 2017 and 2019 cores. This underscores the impact of high temperatures on the preservation of pristine atmospheric signals in ice cores that have significantly impacted the preservation of the atmospheric signal, since temperature values.

5. Conclusion

An ice core drilled at the summit of Holtedahlfonna has previously been used to provide atmospheric and climate conditions about the past 300 years. Before 2005, the site was characterized by moderate summer melting, yet the snow and ice analysed proved to preserve important climate information as well as the main seasonal features. The current warming of the Svalbard archipelago has clearly enhanced glacial mass loss, with a rise in the equilibrium line altitude and a shorter snow season. This study is the first investigating the impact of temperature rise on climate signal preservation within the firn\ice in one of the highest ice fields in Svalbard. The direct effect of higher temperatures has increased summer melt and enhanced meltwater percolation. In this study, we have shown that the climate signal preserved in the ice has been progressively deteriorated. For example, in seven years, the seasonal signal visible in the 2012 core has completely disappeared in the 2019 core, most likely due to increased snow summer melting and water percolation. However, although the $\delta^{18}O$ seasonal signal has disappeared, the overall atmospheric warming signature is still preserved in the ice\firn, suggesting that the site is still suitable for long record paleoclimate reconstruction. However, with the current warming rate of the Svalbard archipelago and the consequent increase in summer melting, Holtedahlfonna and other ice fields at similar altitudes might no longer provide suitable records of the climatic condition. Glaciers worldwide are currently not only losing mass at unprecedented rates, but also the climatic information they contain.

Acknowledgments

This work has been supported by the “Programma di Ricerca in Artico” (PRA, project number PRA2019-0011, Sentinel); by the Svalbard Science Forum/Research Council of Norway through the

Arctic Field Grant call (project ASIHAD, ISSICOS, BIOMASS), by French Polar Institute IPEV (Institut Polaire Français Paul-Emile Victor) science funding (programs 399 and 1192) and the Svalbard Strategic Grant (project C2S3, nr. 257636, SnowNet nr. 295779 and BC3D nr. 283466). This project has received funding from the European Union's Horizon 2020 research and innovation programme under grant agreement no. 689443 via project iCUPE (Integrative and Comprehensive Understanding on Polar Environments). This research has been partially funded by the University of Perugia Research Action no. 5 "Climate, Energy, and Mobility". Cryogrid simulations have been supported by the Nansen Legacy project (Research Council of Norway grant 276730) and SIOS infraNor (Research Council of Norway grant 269927).

Author contribution

AS, EB, FS, JCG, CL, MB, JG, FB, and DC conceived the experiment and collected the samples and wrote the paper with the support of all co-authors; CT, TM, GD and BS analyze the samples; JK provide the field mass balance data and contribute in data interpretation; LSS and TVS provide the model data and atmospheric re-analysis; FdB and MC perform the statistical exercise and contribute in data interpretation. BL and FD contribute to data interpretation. DD and EI provide the data from previous ice core and contribute to data interpretation.

Data availability

The $\delta^{18}O$ data from shallow ice cores will be available at this link (*Zenodo link here*).

Competing interests

The authors declare that they have no conflict of interest.

FIGURES

Figure 1. Location of the drilling site (red star) within the Holtedahlfonna (HDF) ice field as compared to the Ny-Ålesund research village (NyA). Maps from https://toposvalbard.npolar.no (last access: 5th June 2023).

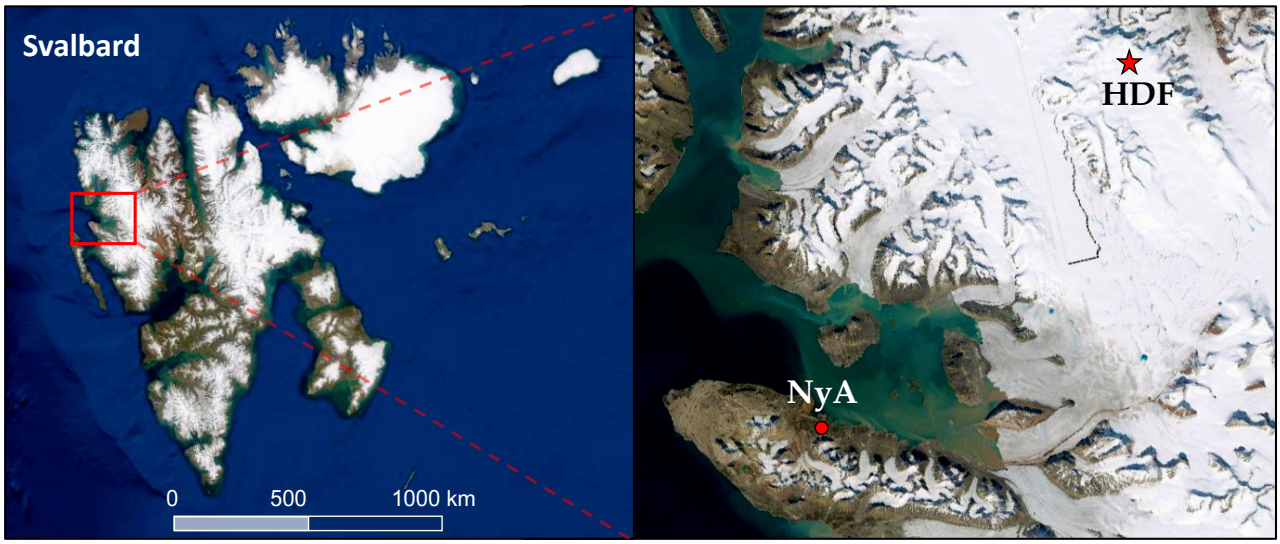

Figure 2. Mass balance measurements, modelled precipitation and snow melt at the drilling site for the period 2004-2019. a) cumulative surface mass balance (SMB) expressed in cm of w.e., b) comparison of modeled total annual precipitation (green – in mm w.e) and modeled melt (red in mm w.e). c-e) net, winter and summer mass balance (cm w.e.) measured at the top of the Holtedahlfonna ice field, respectively.

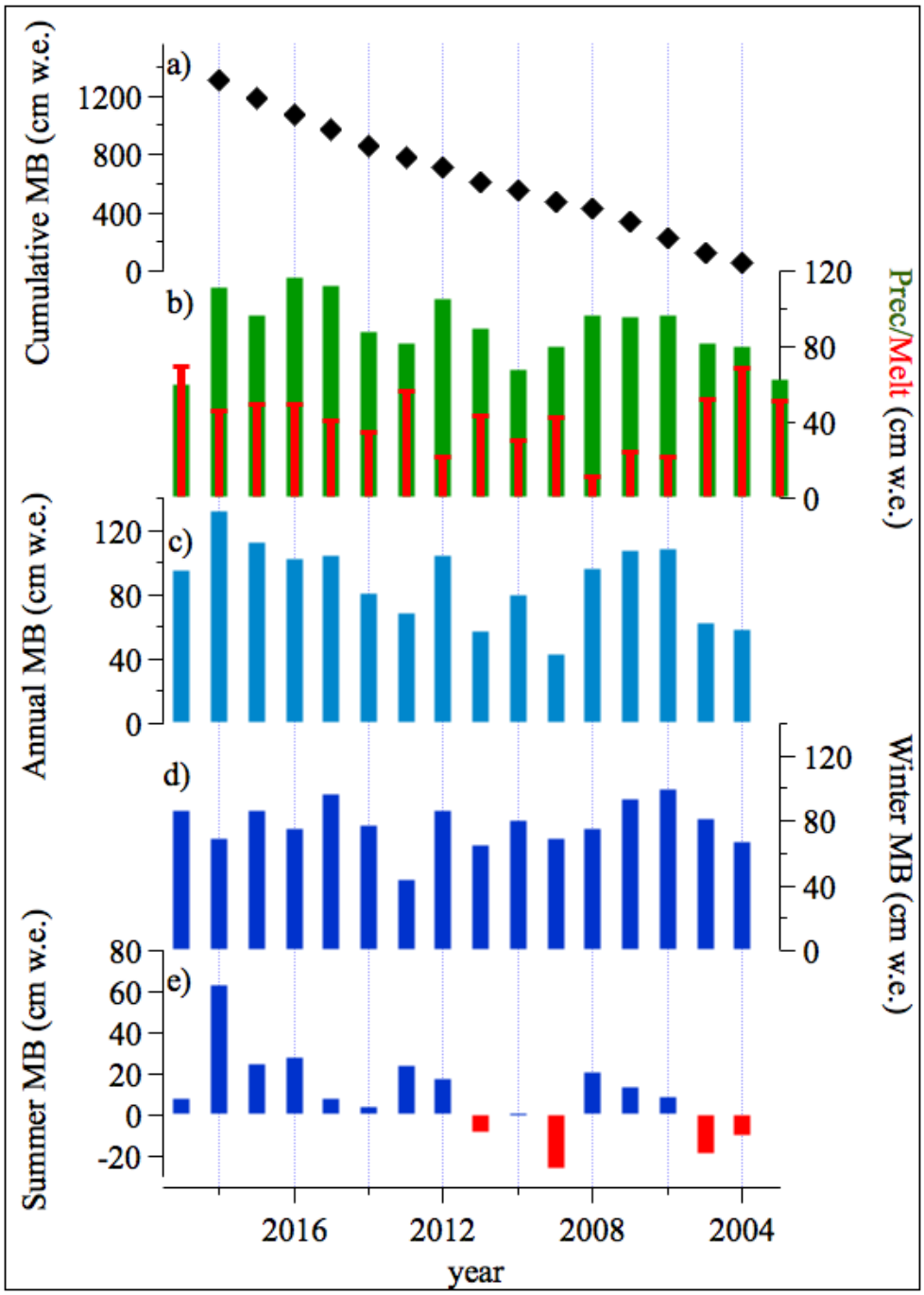

Figure 3. Oxygen stable isotope profiles $\delta^{18}O$ of the shallow cores. The shallow core was aligned by converting the depth to depth expressed in cm of w.e. using the annual mass balance (MB) data. The white and pink colors distinguish different years based on the MB measurements and are reported in the upper panel. The "0 cm" value refers to the last summer snow surface.

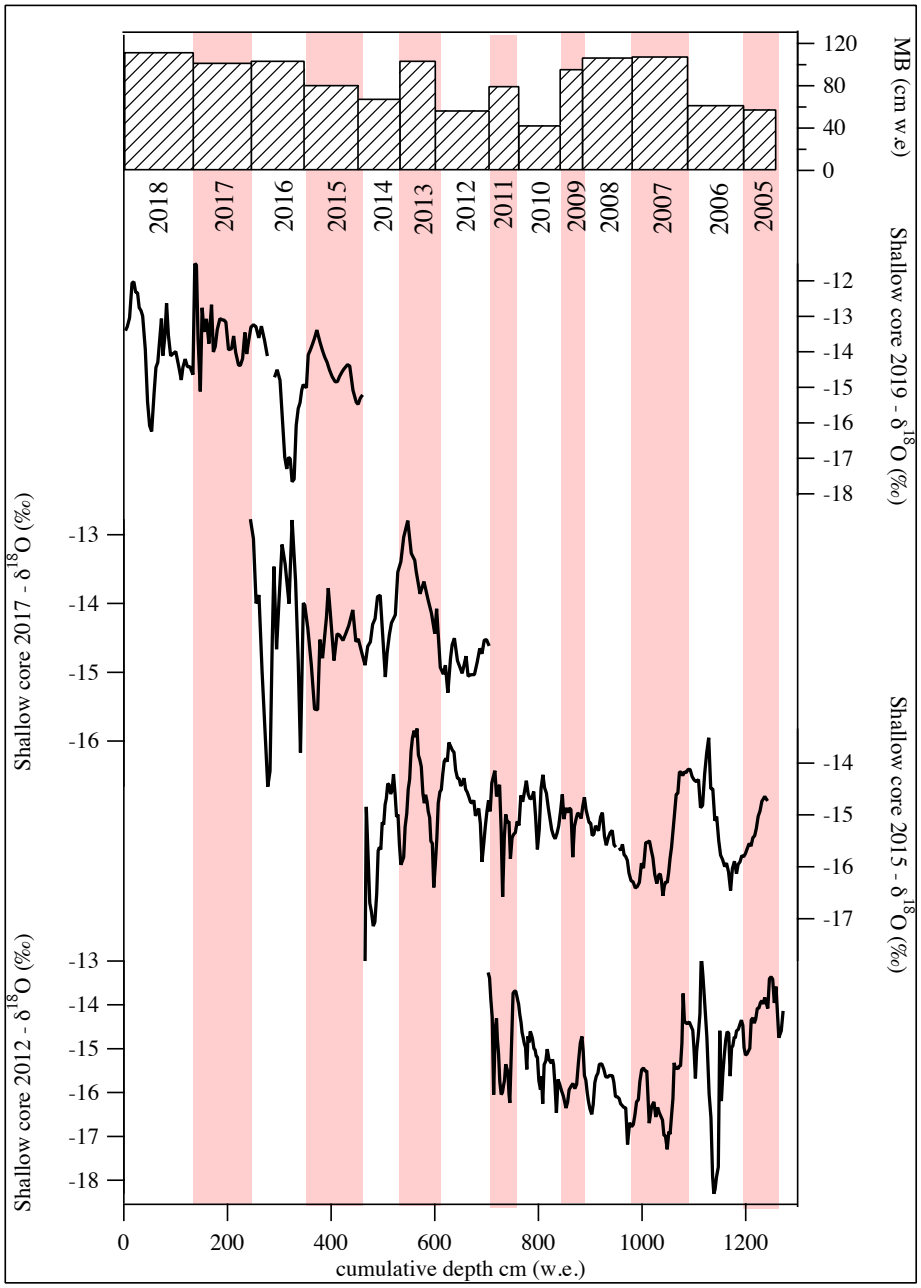

Figure 4. Modeled meteorological conditions at the Holtedahlfonna shallow core drilling site (1150 m a.s.l.) from 1991 to 2019 at seasonal resolution. a) winter (DJF - blue), spring (MAM – green), summer (JJA – red) and fall (SON – brown) temperatures, with increasing trend line for the period investigated. b) annual PDD value (grey). c) annual melting (in mm w.e in red). d) annual total precipitation (in mm w.e. – blue)

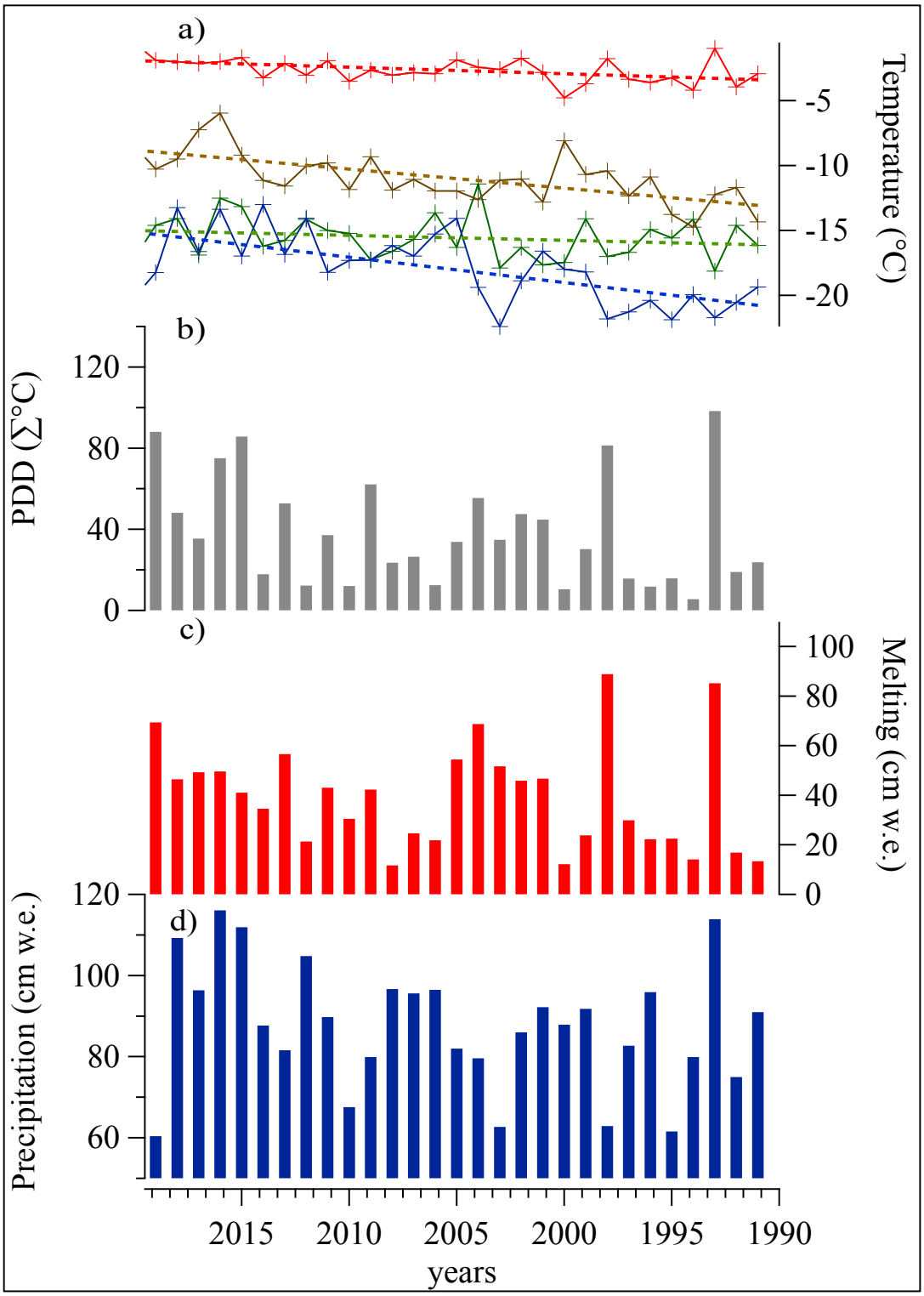

Figure 5. Evolution of the water content in the snowpack at the top of Holtedahlfonna estimated by model simulation between 1990 and 2020. The chart shows the volumetric water content (%) in the snow/firn (white to blue color), surface height evolution (black line), 0° C isotherm (red). Dashed lines show the period covered by the four shallow cores.

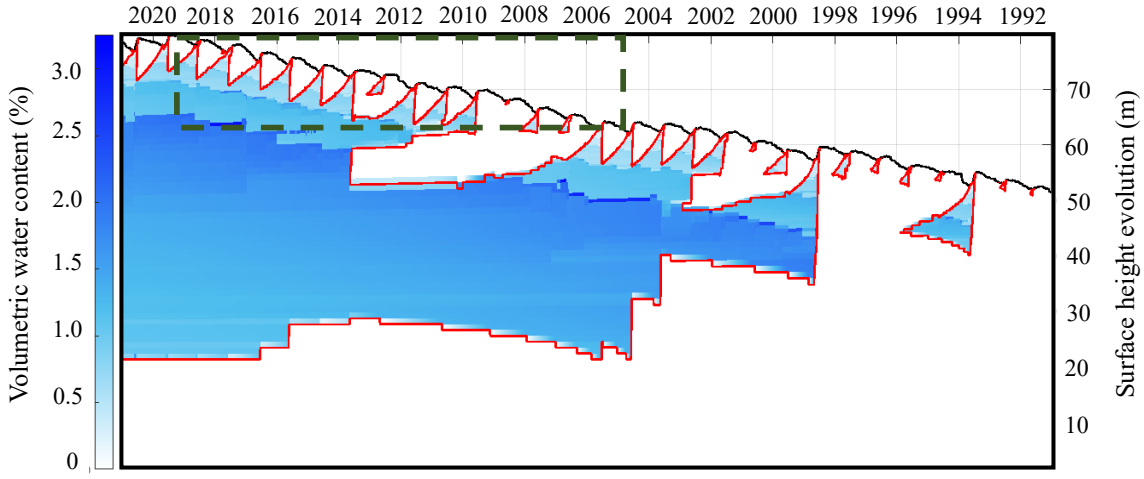

Figure 6. Identification of the annual minimum and maximum values of $\delta^{18}O$ (red and blue points) based on the annual mass balance dating for the four shallow cores (panel a – 2012 core, panel b – 2015 core, panel c – 2017 core, panel d – 2019 core).

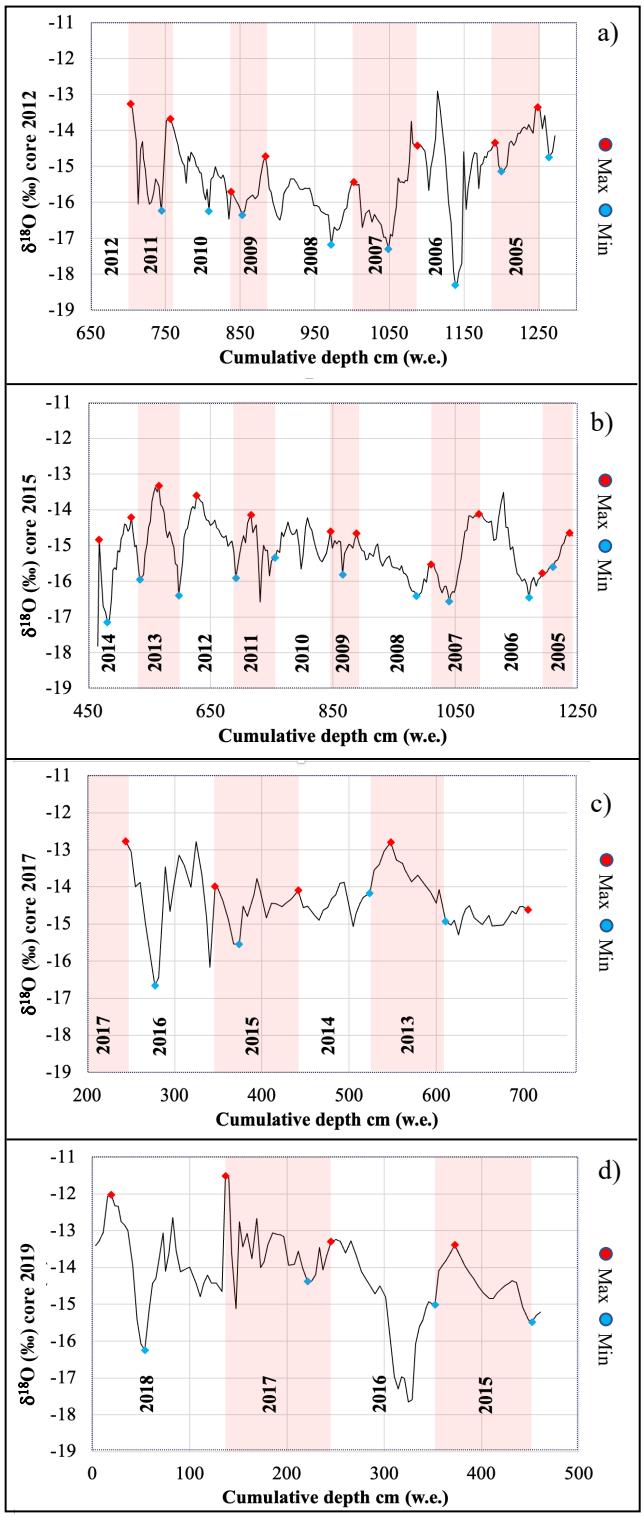

Figure 7. Representation of the slope between the annual maximum and minimum value of $\delta^{18}O$ weighted on the percent difference in the value of $\delta^{18}O$ for each annual mass balance for the four shallow cores. The black line represents the trend of weighted slope change along the years (panel a – 2012 core, panel b – 2015 core, panel c – 2017 core, panel d – 2019 core).

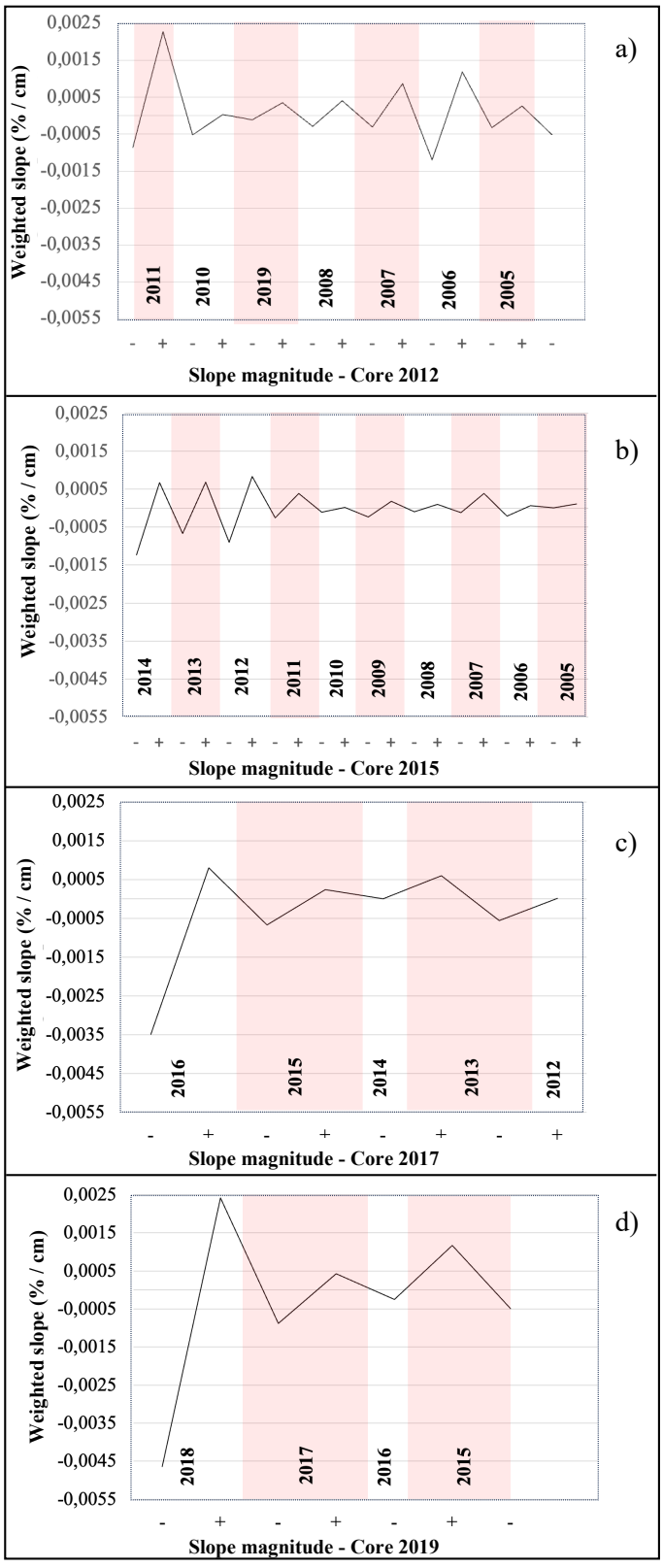

Figure 8. Estimated annual average temperature at the top of Holtedahlfonna ice field (black square) obtained from the monthly atmospheric re-analysis data as describe in section 2.5 and presented in figure S4. The circles representing the $\delta^{18}O$ signal of the four shallow cores (black circle for the 2012 core, green circles for the 2015 core, blue circle for the 2017 core and red circle for the 2019 core).

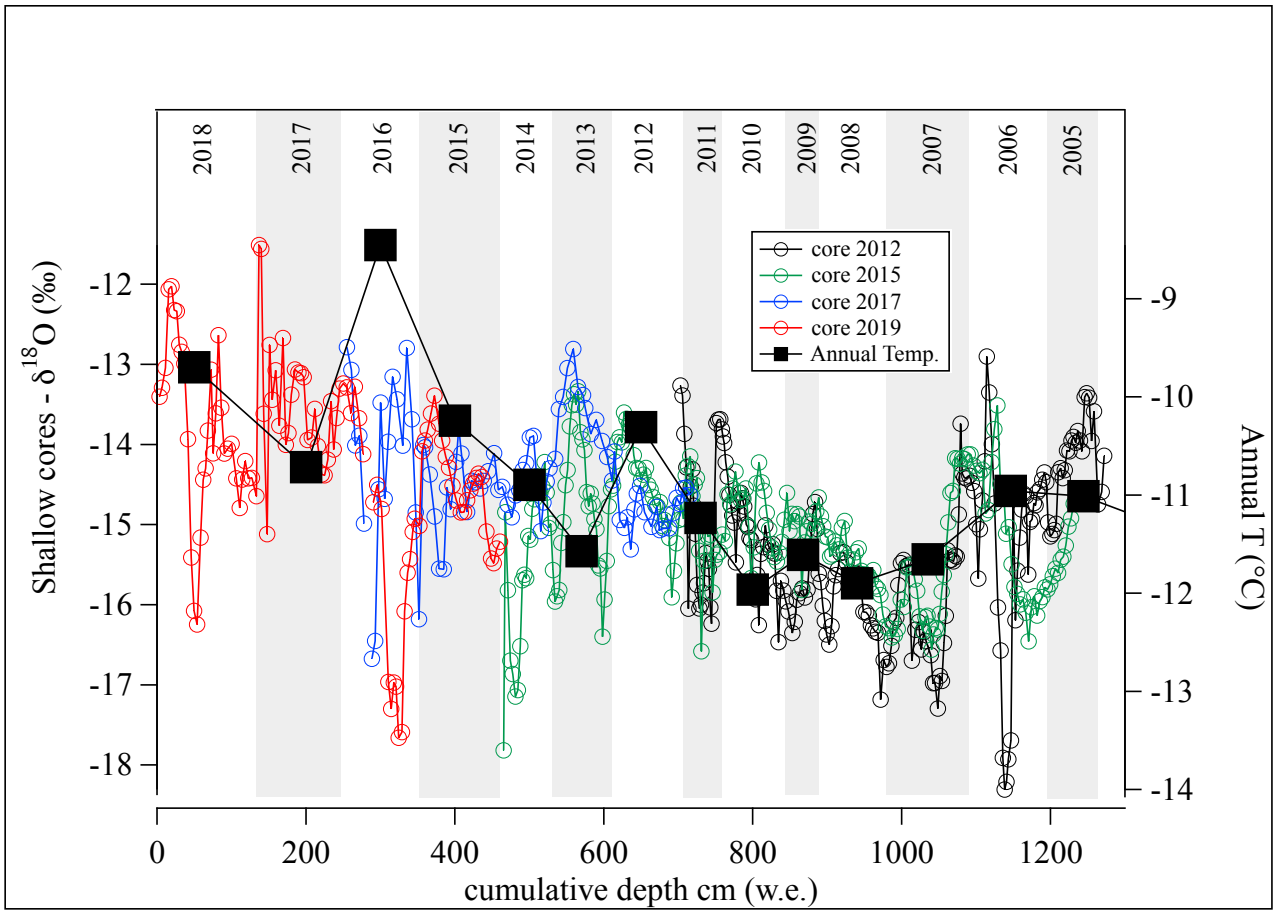

TABLES

Table 1. Shallow ice core descriptions. The table reports the length expressed in cm and in water equivalent (w.e.) and the estimated (Est. start year\Est. end year) time coverage. The average density of the cores is also reported.

Core ID	Length (cm)	Length (cm w.e.)	Ave density (kgL^{-1})	Est. Start year	Est. End year	Drilling period	Reference
2019	769	461	0.60	2018	2012	April 2019	This work
2017	736	466	0.63	2016	2010	April 2017	*Burgay et a. 2017*
2015	1185	832	0.70	2014	2005	May 2015	*Ruppel et al. 2017*
2012	954	575	0.60	2011	2005	April 2012	*Spolaor et al. 2013*

679
680
681 **REFERENCES**
682

683 Arienzo, M. M., Legrand, M., Preunkert, S., Stohl, A., Chellman, N., Eckhardt, S., Gleason, K. E.,
684 and McConnell, J. R.: Alpine Ice-Core Evidence of a Large Increase in Vanadium and
685 Molybdenum Pollution in Western Europe During the 20th Century, Journal of Geophysical
686 Research: Atmospheres, 126, https://doi.org/10.1029/2020JD033211, 2021.
687 Avak, S. E., Trachsel, J. C., Edebeli, J., Brütsch, S., Bartels-Rausch, T., Schneebeli, M.,
688 Schwikowski, M., and Eichler, A.: Melt-Induced Fractionation of Major Ions and Trace
689 Elements in an Alpine Snowpack, J Geophys Res Earth Surf, 124, 1647–1657,
690 https://doi.org/10.1029/2019JF005026, 2019.
691 Barbaro, E., Spolaor, A., Karroca, O., Park, K.-T., Martma, T., Isaksson, E., Kohler, J., Gallet, J. C.,
692 Bjorkman, M. P., Cappelletti, D., Spreen, G., Zangrando, R., Barbante, C., and Gambaro, A.:
693 Free amino acids in the Arctic snow and ice core samples: Potential markers for paleoclimatic
694 studies, Science of the Total Environment, 607–608,
695 https://doi.org/10.1016/j.scitotenv.2017.07.041, 2017.
696 Beaudon, E., Moore, J. C., Martma, T., Pohjola, V. A., van de Wal, R. S. W., Kohler, J., and
697 Isaksson, E.: Lomonosovfonna and Holtedahlfonna ice cores reveal east–west disparities of the
698 Spitsbergen environment since AD 1700, Journal of Glaciology, 59, 1069–1083,
699 https://doi.org/10.3189/2013JoG12J203, 2017.
700 Bengtsson, L., Andrae, U., Aspelien, T., Batrak, Y., Calvo, J., de Rooy, W., Gleeson, E., Hansen-
701 Sass, B., Homleid, M., Hortal, M., Ivarsson, K.-I., Lenderink, G., Niemelä, S., Nielsen, K. P.,
702 Onvlee, J., Rontu, L., Samuelsson, P., Muñoz, D. S., Subias, A., Tijm, S., Toll, V., Yang, X., and
703 Køltzow, M. Ø.: The HARMONIE–AROME Model Configuration in the ALADIN–HIRLAM
704 NWP System, Mon Weather Rev, 145, 1919–1935, https://doi.org/10.1175/MWR-D-16-0417.1,
705 2017.
706 Boers, N.: Early-warning signals for Dansgaard-Oeschger events in a high-resolution ice core
707 record, Nat Commun, 9, 2556, https://doi.org/10.1038/s41467-018-04881-7, 2018.
708 Bohleber, P., Roman, M., Šala, M., Delmonte, B., Stenni, B., and Barbante, C.: Two-dimensional
709 impurity imaging in deep Antarctic ice cores: snapshots of three climatic periods and
710 implications for high-resolution signal interpretation, Cryosphere, 15, 3523–3538,
711 https://doi.org/10.5194/tc-15-3523-2021, 2021.
712 Bonne, J.-L., Steen-Larsen, H. C., Risi, C., Werner, M., Sodemann, H., Lacour, J.-L., Fettweis, X.,
713 Cesana, G., Delmotte, M., Cattani, O., Vallelonga, P., Kjær, H. A., Clerbaux, C.,
714 Sveinbjörnsdóttir, Á. E., and Masson-Delmotte, V.: The summer 2012 Greenland heat wave: In
715 situ and remote sensing observations of water vapor isotopic composition during an atmospheric
716 river event, Journal of Geophysical Research: Atmospheres, 120, 2970–2989,
717 https://doi.org/10.1002/2014JD022602, 2015.
718 Burgay, F., Barbaro, E., Cappelletti, D., Turetta, C., Gallet, J.-C., Isaksson, E., Stenni, B., Dreossi,
719 G., Scoto, F., Barbante, C., and Spolaor, A.: First discrete iron(II) records from Dome C
720 (Antarctica) and the Holtedahlfonna glacier (Svalbard), Chemosphere, 267, 129335,
721 https://doi.org/https://doi.org/10.1016/j.chemosphere.2020.129335, 2021.
722 Cisek, M., Makuch, P., and Petelski, T.: Comparison of meteorological conditions in Svalbard
723 fjords: Hornsund and Kongsfjorden, Oceanologia, 59, 413–421,
724 https://doi.org/10.1016/j.oceano.2017.06.004, 2017.
725 Dahe, Q., Mayewski, P. A., Wake, C. P., Shichang, K., Jiawen, R., Shugui, H., Tandong, Y.,
726 Qinzhao, Y., Zhefan, J., and Desheng, M.: Evidence for recent climate change from ice cores in
727 the central Himalaya, Ann Glaciol, 31, 153–158, https://doi.org/10.3189/172756400781819789,
728 2000.

729 Dahlke, S. and Maturilli, M.: Contribution of atmospheric advection to the amplified winter
730 warming in the arctic north atlantic region, Advances in meteorology,
731 https://doi.org/10.1155/2017/4928620, 2017.
732 Dahlke, S., Hughes, N. E., Wagner, P. M., Gerland, S., Wawrzyniak, T., Ivanov, B., and Maturilli,
733 M.: The observed recent surface air temperature development across Svalbard and concurring
734 footprints in local sea ice cover, International Journal of Climatology, 40, 5246–5265,
735 https://doi.org/https://doi.org/10.1002/joc.6517, 2020.
736 Divine, D., Isaksson, E., Martma, T., Meijer, H. A. J., Moore, J., Pohjola, V., van de Wal, R. S. W.,
737 and Godtliebsen, F.: Thousand years of winter surface air temperature variations in Svalbard and
738 northern Norway reconstructed from ice-core data, Polar Res, 30, 7379,
739 https://doi.org/10.3402/polar.v30i0.7379, 2011.
740 Førland, E. J., Isaksen, K., Lutz, J., Hanssen-Bauer, I., Schuler, T. V., Dobler, A., Gjelten, H. M.,
741 and Vikhamar-Schuler, D.: Measured and Modeled Historical Precipitation Trends for Svalbard,
742 J Hydrometeorol, 21, 1279–1296, https://doi.org/10.1175/JHM-D-19-0252.1, 2020.
743 Gabrielli, P., Barbante, C., Bertagna, G., Bertó, M., Binder, D., Carton, A., Carturan, L., Cazorzi,
744 F., Cozzi, G., Dalla Fontana, G., Davis, M., De Blasi, F., Dinale, R., Dragà, G., Dreossi, G.,
745 Festi, D., Frezzotti, M., Gabrieli, J., Galos, S. P., Ginot, P., Heidenwolf, P., Jenk, T. M.,
746 Kehrwald, N., Kenny, D., Magand, O., Mair, V., Mikhalenko, V., Lin, P. N., Oeggl, K., Piffer,
747 G., Rinaldi, M., Schotterer, U., Schwikowski, M., Seppi, R., Spolaor, A., Stenni, B., Tonidandel,
748 D., Uglietti, C., Zagorodnov, V., Zanoner, T., and Zennaro, P.: Age of the Mt. Ortles ice cores,
749 the Tyrolean Iceman and glaciation of the highest summit of South Tyrol since the Northern
750 Hemisphere Climatic Optimum, Cryosphere, 10, 2779–2797, https://doi.org/10.5194/tc-10-2779-
751 2016, 2016.
752 Geyman, E. C., J. J. van Pelt, W., Maloof, A. C., Aas, H. F., and Kohler, J.: Historical glacier
753 change on Svalbard predicts doubling of mass loss by 2100, Nature, 601, 374–379,
754 https://doi.org/10.1038/s41586-021-04314-4, 2022.
755 Goto-Azuma, K., S. Kohshima, T., Kameda, S., Takahashi, O., Watanabe, Y. F., and Hagen., and J.
756 O.: An ice-core chemistry record from Snøfjellafonna, northwestern Spitsbergen, Ann. Glaciol.,
757 21, 213–218, 1995.
758 Hersbach, H., Bell, B., Berrisford, P., Hirahara, S., Horányi, A., Muñoz-Sabater, J., Nicolas, J.,
759 Peubey, C., Radu, R., Schepers, D., Simmons, A., Soci, C., Abdalla, S., Abellan, X., Balsamo,
760 G., Bechtold, P., Biavati, G., Bidlot, J., Bonavita, M., Chiara, G., Dahlgren, P., Dee, D.,
761 Diamantakis, M., Dragani, R., Flemming, J., Forbes, R., Fuentes, M., Geer, A., Haimberger, L.,
762 Healy, S., Hogan, R. J., Hólm, E., Janisková, M., Keeley, S., Laloyaux, P., Lopez, P., Lupu, C.,
763 Radnoti, G., Rosnay, P., Rozum, I., Vamborg, F., Villaume, S., and Thépaut, J.: The ERA5
764 global reanalysis, Quarterly Journal of the Royal Meteorological Society, 146, 1999–2049,
765 https://doi.org/10.1002/qj.3803, 2020.
766 Hoffmann, G., Ramirez, E., Taupin, J. D., Francou, B., Ribstein, P., Delmas, R., Dürr, H., Gallaire,
767 R., Simões, J., Schotterer, U., Stievenard, M., and Werner, M.: Coherent isotope history of
768 Andean ice cores over the last century, Geophys Res Lett, 30, 2002GL014870,
769 https://doi.org/10.1029/2002GL014870, 2003.
770 Isaksen, K., Nordli, Ø., Førland, E. J., Łupikasza, E., Eastwood, S., and Niedźwiedź, T.: Recent
771 warming on Spitsbergen—Influence of atmospheric circulation and sea ice cover, Journal of
772 Geophysical Research: Atmospheres, 121, 11, 911–913, 931,
773 https://doi.org/10.1002/2016JD025606, 2016.
774 Isaksen, K., Nordli, Ø., Ivanov, B., Køltzow, M. A. Ø., Aaboe, S., Gjelten, H. M., Mezghani, A.,
775 Eastwood, S., Førland, E., Benestad, R. E., Hanssen-Bauer, I., Brækkan, R., Sviashchennikov,
776 P., Demin, V., Revina, A., and Karandasheva, T.: Exceptional warming over the Barents area,
777 Sci Rep, 12, 9371, https://doi.org/10.1038/s41598-022-13568-5, 2022.
778 Isaksson, E., Hermanson, M., Hicks, S., Igarashi, M., Kamiyama, K., Moore, J., Motoyama, H.,
779 Muir, D., Pohjola, V., Vaikmäe, R., van de Wal, R. S. W., and Watanabe, O.: Ice cores from

Svalbard—useful archives of past climate and pollution history, Physics and Chemistry of the Earth, Parts A/B/C, 28, 1217–1228, https://doi.org/10.1016/j.pce.2003.08.053, 2003.
Isaksson, E., Kekonen, T., Moore, J., and Mulvaney, R.: The methanesulfonic acid (MSA) record in a Svalbard ice core, Ann. Glaciol., 42, 345–351, 2005.
Kohler, J.: Mass balance for glaciers near Ny-Ålesund [Data set]. Norwegian Polar Institute, 2013.
Lind, S., Ingvaldsen, R. B., and Furevik, T.: Arctic warming hotspot in the northern Barents Sea linked to declining sea-ice import, Nat Clim Chang, 8, 634–639, https://doi.org/10.1038/s41558-018-0205-y, 2018.
Matoba, S., Narita, H., Motoyama, H., Kamiyama, K., and Watanabe, O.: Ice core chemistry of Vestfonna Ice Cap in Svalbard, Norway, Journal of Geophysical Research: Atmospheres, 107, ACH 19-1-ACH 19-7, https://doi.org/10.1029/2002JD002205, 2002.
Maturilli, M., Herber, A., and König-Langlo, G.: Climatology and time series of surface meteorology in Ny-Ålesund, Svalbard, Earth Syst. Sci. Data, 5, 155–163, https://doi.org/10.5194/essd-5-155-2013, 2013.
Nuth, C., Schuler, T. V., Kohler, J., Altena, B., and Hagen, J. O.: Estimating the long-term calving flux of Kronebreen, Svalbard, from geodetic elevation changes and mass-balance modeling, Journal of Glaciology, 58, 119–133, https://doi.org/10.3189/2012JoG11J036, 2017.
Østby, T. I., Schuler, T. v, Hagen, J. O., Hock, R., Kohler, J., and Reijmer, C. H.: Diagnosing the decline in climatic mass balance of glaciers in Svalbard over 1957–2014, Cryosphere, 11, 191–215, https://doi.org/10.5194/tc-11-191-2017, 2017.
Peeters, B., Pedersen, Å. Ø., Loe, L. E., Isaksen, K., Veiberg, V., Stien, A., Kohler, J., Gallet, J.-C., Aanes, R., and Hansen, B. B.: Spatiotemporal patterns of rain-on-snow and basal ice in high Arctic Svalbard: detection of a climate-cryosphere regime shift, Environmental Research Letters, 14, 015002, https://doi.org/10.1088/1748-9326/aaefb3, 2019.
van Pelt, W. J. J., Kohler, J., Liston, G. E., Hagen, J. O., Luks, B., Reijmer, C. H., and Pohjola, V. A.: Multidecadal climate and seasonal snow conditions in Svalbard, J Geophys Res Earth Surf, 121, 2100–2117, https://doi.org/https://doi.org/10.1002/2016JF003999, 2016.
van Pelt, W., Pohjola, V., Pettersson, R., Marchenko, S., Kohler, J., Luks, B., Hagen, J. O., Schuler, T. v, Dunse, T., Noël, B., and Reijmer, C.: A long-term dataset of climatic mass balance, snow conditions, and runoff in Svalbard (1957–2018), Cryosphere, 13, 2259–2280, https://doi.org/10.5194/tc-13-2259-2019, 2019.
Pohjola, V. A., Moore, J. C., Isaksson, E., Jauhiainen, T., Van de Wal, R. S. W., Martma, T., Meijer, H. A. J., and Vaikmäe, R.: Effect of periodic melting on geochemical and isotopic signals in an ice core from Lomonosovfonna, Svalbard, J. Geophys. Res. Atmos., 107, 1–14, 2002.
Rantanen, M., Karpechko, A. Yu., Lipponen, A., Nordling, K., Hyvärinen, O., Ruosteenoja, K., Vihma, T., and Laaksonen, A.: The Arctic has warmed nearly four times faster than the globe since 1979, Commun Earth Environ, 3, 168, https://doi.org/10.1038/s43247-022-00498-3, 2022.
Ruppel, M. M., Soares, J., Gallet, J.-C., Isaksson, E., Martma, T., Svensson, J., Kohler, J., Pedersen, C. A., Manninen, S., Korhola, A., and Ström, J.: Do contemporary (1980–2015) emissions determine the elemental carbon deposition trend at Holtedahlfonna glacier, Svalbard?, Atmos Chem Phys, 17, 12779–12795, https://doi.org/10.5194/acp-17-12779-2017, 2017.
Salzano, R., Cerrato, R., Scoto, F., Spolaor, A., Valentini, E., Salvadore, M., Esposito, G., Sapio, S., Taramelli, A., and Salvatori, R.: Detection of Winter Heat Wave Impact on Surface Runoff in a Periglacial Environment (Ny-Ålesund, Svalbard), Remote Sens (Basel), 15, 4435, https://doi.org/10.3390/rs15184435, 2023.
Schuler, T. v, Kohler, J., Elagina, N., Hagen, J. O. M., Hodson, A. J., Jania, J. A., Kääb, A. M., Luks, B., Małecki, J., Moholdt, G., Pohjola, V. A., Sobota, I., and van Pelt, W. J. J.: Reconciling Svalbard Glacier Mass Balance, Front Earth Sci (Lausanne), 8, 2020.

Schwikowski, M., Döscher, A., Gäggeler, H. W., and Schotterer, U.: Anthropogenic versus natural sources of atmospheric sulphate from an Alpine ice core, Tellus B: Chemical and Physical Meteorology, 51, 938, https://doi.org/10.3402/tellusb.v51i5.16506, 1999.

Schyberg, H. , Yang, X. , Koltzow, M. , Amstrup, B. , ., Bakketun, B., Bazile, E. , Bojarova, J. , Box, J. , Dahlgren, P. , Hagelin, S. , Homleid, M. , Horanyi, A. , Hoyer, J. , Johansson, K. M. , Kornich, H. , le Moigne, P. , Lindskog, M. , Manninen, T. , Nielsen Englyst, P. , and and Wang, Z.: Arctic regional reanalysis on single levels from 1991 to present, , 2020.

Scoto, F., Sadatzki, H., Maffezzoli, N., Barbante, C., Gagliardi, A., Varin, C., Vallelonga, P., Gkinis, V., Dahl-Jensen, D., Kjær, H. A., Burgay, F., Saiz-Lopez, A., Stein, R., and Spolaor, A.: Sea ice fluctuations in the Baffin Bay and the Labrador Sea during glacial abrupt climate changes, Proceedings of the National Academy of Sciences, 119, e2203468119, https://doi.org/10.1073/pnas.2203468119, 2022.

Serreze, M. C. and Barry, R. G.: Processes and impacts of Arctic amplification: A research synthesis, Glob Planet Change, 77, 85–96, https://doi.org/http://dx.doi.org/10.1016/j.gloplacha.2011.03.004, 2011.

Sigl, M., McConnell, J. R., Toohey, M., Curran, M., Das, S. B., Edwards, R., Isaksson, E., Kawamura, K., Kipfstuhl, S., Kruger, K., Layman, L., Maselli, O. J., Motizuki, Y., Motoyama, H., Pasteris, D. R., and Severi, M.: Insights from Antarctica on volcanic forcing during the Common Era, Nature Clim. Change, 4, 693–697, https://doi.org/10.1038/nclimate2293 http://www.nature.com/nclimate/journal/v4/n8/abs/nclimate2293.html#supplementary-information, 2014.

Sobota, I., Weckwerth, P., and Grajewski, T.: Rain-On-Snow (ROS) events and their relations to snowpack and ice layer changes on small glaciers in Svalbard, the high Arctic, J Hydrol (Amst), 590, 125279, https://doi.org/https://doi.org/10.1016/j.jhydrol.2020.125279, 2020.

Spolaor, A., Gabrieli, J., Martma, T., Kohler, J., Björkman, M. B., Isaksson, E., Varin, C., Vallelonga, P., Plane, J. M. C., and Barbante, C.: Sea ice dynamics influence halogen deposition to Svalbard, Cryosphere, 7, https://doi.org/10.5194/tc-7-1645-2013, 2013.

Spolaor, A., Varin, C., Pedeli, X., Christille, J. M., Kirchgeorg, T., Giardi, F., Cappelletti, D., Turetta, C., Cairns, W. R. L., Gambaro, A., Bernagozzi, A., Gallet, J. C., Björkman, M. P., and Barbaro, E.: Source, timing and dynamics of ionic species mobility in the Svalbard annual snowpack, Science of The Total Environment, 751, 141640, https://doi.org/https://doi.org/10.1016/j.scitotenv.2020.141640, 2021.

Steffensen, J. P., Andersen, K. K., Bigler, M., Clausen, H. B., Dahl-Jensen, D., Fischer, H., Goto-Azuma, K., Hansson, M., Johnsen, S. J., Jouzel, J., Masson-Delmotte, V., Popp, T., Rasmussen, S. O., Röthlisberger, R., Ruth, U., Stauffer, B., Siggaard-Andersen, M.-L., Sveinbjörnsdóttir, Á. E., Svensson, A., and White, J. W. C.: High-Resolution Greenland Ice Core Data Show Abrupt Climate Change Happens in Few Years, Science (1979), 321, 680–684, 2008.

Steffensen Schmidt, L., Schuler, T. V, Thomas, E. E., and Westermann, S.: Meltwater runoff and glacier mass balance in the high Arctic: 1991–2022 simulations for Svalbard, EGUsphere, 2023, 1–32, https://doi.org/10.5194/egusphere-2022-1409, 2023.

Stenni, B., Curran, M. A. J., Abram, N. J., Orsi, A., Goursaud, S., Masson-Delmotte, V., Neukom, R., Goosse, H., Divine, D., van Ommen, T., Steig, E. J., Dixon, D. A., Thomas, E. R., Bertler, N. A. N., Isaksson, E., Ekaykin, A., Werner, M., and Frezzotti, M.: Antarctic climate variability on regional and continental scales over the last 2000 years, Clim. Past, 13, 1609–1634, https://doi.org/10.5194/cp-13-1609-2017, 2017.

Thompson, L. G., Yao, T., Davis, M. E., Mosley-Thompson, E., Wu, G., Porter, S. E., Xu, B., Lin, P.-N., Wang, N., Beaudon, E., Duan, K., Sierra-Hernández, M. R., and Kenny, D. v.: Ice core records of climate variability on the Third Pole with emphasis on the Guliya ice cap, western Kunlun Mountains, Quat Sci Rev, 188, 1–14, https://doi.org/10.1016/j.quascirev.2018.03.003, 2018.

Thompson, L. G., Davis, M. E., Mosley-Thompson, E., Porter, S. E., Corrales, G. V., Shuman, C. A., and Tucker, C. J.: The impacts of warming on rapidly retreating high-altitude, low-latitude glaciers and ice core-derived climate records, Glob Planet Change, 203, 103538, https://doi.org/10.1016/j.gloplacha.2021.103538, 2021.
Vecchiato, M., Gambaro, A., Kehrwald, N. M., Ginot, P., Kutuzov, S., Mikhalenko, V., and Barbante, C.: The Great Acceleration of fragrances and PAHs archived in an ice core from Elbrus, Caucasus, Sci Rep, 10, 10661, https://doi.org/10.1038/s41598-020-67642-x, 2020.
Wendl, I. A., Eichler, A., Isaksson, E., Martma, T., and Schwikowski, M.: 800-year ice-core record of nitrogen deposition in Svalbard linked to ocean productivity and biogenic emissions, Atmos. Chem. Phys., 15, 7287–7300, https://doi.org/10.5194/acp-15-7287-2015, 2015.
Westermann, S., Ingeman-Nielsen, T., Scheer, J., Aalstad, K., Aga, J., Chaudhary, N., Etzelmüller, B., Filhol, S., Kääb, A., Renette, C., Schmidt, L. S., Schuler, T. V., Zweigel, R. B., Martin, L., Morard, S., Ben-Asher, M., Angelopoulos, M., Boike, J., Groenke, B., Miesner, F., Nitzbon, J., Overduin, P., Stuenzi, S. M., and Langer, M.: The CryoGrid community model (version 1.0) – a multi-physics toolbox for climate-driven simulations in the terrestrial cryosphere, Geosci Model Dev, 16, 2607–2647, https://doi.org/10.5194/gmd-16-2607-2023, 2023.
Wickström, S., Jonassen, M. O., Cassano, J. J., and Vihma, T.: Present Temperature, Precipitation, and Rain-on-Snow Climate in Svalbard, Journal of Geophysical Research: Atmospheres, 125, e2019JD032155, https://doi.org/https://doi.org/10.1029/2019JD032155, 2020.
Wolff, E. W., Barbante, C., Becagli, S., Bigler, M., Boutron, C. F., Castellano, E., de Angelis, M., Federer, U., Fischer, H., and Fundel, F.: Changes in environment over the last 800,000 years from chemical analysis of the EPICA Dome C ice core, Quaternary Sci Rev, 29, 285–295, 2010.
Zdanowicz, C. M., Proemse, B. C., Edwards, R., Feiteng, W., Hogan, C. M., Kinnard, C., and Fisher, D.: Historical black carbon deposition in the Canadian High Arctic: a >250-year long ice-core record from Devon Island, Atmos Chem Phys, 18, 12345–12361, https://doi.org/10.5194/acp-18-12345-2018, 2018.